RSC Advances

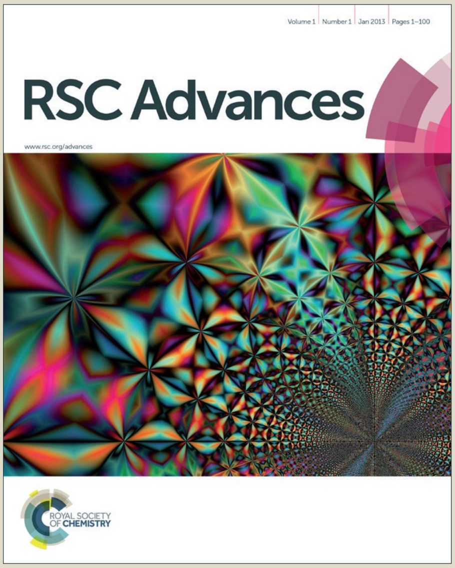

Journal Name

ARTICLE

High-Efficiency Self-Healing Materials Based on Supramolecular Polymer Networks

Received 00th January 20xx,
Accepted 00th January 20xx

DOI: 10.1039/x0xx00000x

www.rsc.org/

Chih-Chia Cheng*[a], Feng-Chih Chang[b], Jem-Kun Chen[c], Tzu-Yin Wang[b], Duu-Jong Lee[d,e]

Supramolecular polymers, a combination of secondary interactions and a polymer material, can be used to control supramolecular self-assembly in a polymeric matrix; these materials exhibit unique stimuli-responsiveness and self-healing properties making them highly attractive for various applications. Herein, we developed a novel supramolecular polyurea containing a urea-cytosine (UrCy) quadruple hydrogen bonding moiety that undergoes a dynamic healing mechanism, "supramolecular polymer networks (SPN)", and rapidly repairs after damage under mild conditions. Interestingly, this newly-developed material can also self-heal at room temperature without external intervention, as evidenced by repeated restoration of mechanical properties. Given its simplicity, efficiency and reliability, this material offers a unique paradigm for developing SPN-based self-healing materials.

Introduction

In recent years, bioinspired materials have become a hugely important topic in polymer science due to their ability to spontaneously heal when damaged; however, it is necessary to improve the long-term durability and lifetime of these materials.[1-3] Like human skin, self-healing polymers can self-repair microscopic damage,[4] and it is also easy to modify the functional structures within self-healing polymers.[5,6] Many research groups have begun to explore the wide range of potential applications for self-healing polymers, such as self-healing thermosetting materials,[7–9] electrical conductors[10–13] and tissue engineering.[14,15] Although there has been significant progress in self-healing materials over the last few years, it is difficult to create multi-functional polymers with excellent healing properties, as traditional polymers are vulnerable to damage and not easy to restore to their original state due to complicated entanglement of the polymer chains. Therefore, the challenge remains to design effective synthetic routes for self-healing polymers that exhibit finely-tuned dynamic behavior with rapid transition times.

In an attempt to resolve the issues described above, stimuli-responsive systems have attracted a great deal of attention in the field of self-healing materials due to their ability to allow precise control over the healing process, as they respond to changes in their internal and external environments.[16,17] Several stimuli-responsive self-healing polymers have been developed as promising intelligent materials with outstanding physical properties, through incorporation of microencapsulated[18] or photosensitive[8,9] healing agents, dynamic covalent bonds,[6,19-23] coordination complexes[24,25] or reversible non-covalent bonding[7,12,26-34] into the polymer matrices. Nevertheless, the sustainability and effectiveness of these approaches have been consistently limited by a lack of understanding regarding the dynamic response of these materials during spontaneous healing processes,[35] and many challenges still remain in the construction of an appropriate system that can simultaneously improve both stimuli-responsiveness and self-healing abilities. As far as the above-mentioned desirable characteristics are concerned, supramolecular polymer networks (SPN) have been confirmed to undergo transient physical interactions that efficiently promote polymer self-assembly, and their polymeric conformation and dynamic behavior can be directly manipulated to create a variety of multifunctional polymers.[36] The introduction of supramolecular interactions in synthetic self-healing polymers may be a promising approach towards the development of a new generation of stimuli-sensitive materials, which may enable the formation of a physically cross-linked structure to obtain rapid and stable response properties under different environmental conditions, and thus increase the reliability and longevity of the SPN polymer. Therefore, polymers constructed using different types of noncovalent interactions may be able to bind with the building blocks of SPNs to achieve the required qualities within self-healing polymers.

---

[a] Graduate Institute of Applied Science and Technology, National Taiwan University of Science and Technology, Taipei 10607, Taiwan. E-mail: cccheng@mail.ntust.edu.tw

[b] Institute of Applied Chemistry, National Chiao Tung University, Hsin Chu 30050, Taiwan.

[c] Department of Materials Science and Engineering, National Taiwan University of Science and Technology, Taipei 10607, Taiwan.

[d] Department of Chemical Engineering, National Taiwan University, Taipei 10617, Taiwan.

[e] Department of Chemical Engineering, National Taiwan University of Science and Technology, Taipei 10607, Taiwan.

Electronic Supplementary Information (ESI) available: synthetic procedures, structural characterizations, general materials and instrumentation used in this work are described in more detail in Supplementary Information.. See DOI: 10.1039/x0xx00000x

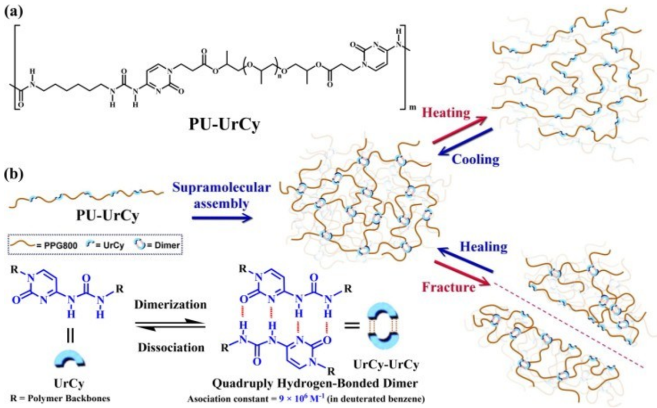

Scheme 1. **(a)** Chemical structure of PU-UrCy. **(b)** Self-healing mechanism for the network formed by thermal and stretching triggering of the hydrogen-bonded UrCy dimer.

Recently, the incorporation of hydrogen bonding supramolecular assembly within polymer structures has been developed, since the strength of the hydrogen bonds can be easily tuned by altering the donor (D) and acceptor (A) sites to produce the desired polymer-like properties without the need for covalent polymerization.[37,38] Hailes and co-workers developed a form of DDAA arrays based on a ureido-substituted cytosine (UrCy) with a high association constant ($K_a = 9 \times 10^6$ M^{-1} in deuterated benzene).[39] Incorporation of self-complementary UrCy units into the polymer chain ends facilitated the formation of ordered structures and resulted in superior physical properties.[40,41] These results were ascribed to close-packing of the UrCy end-groups transferring into hard domains, which can aid the supramolecular binding motif in the bulk state and plays a critical role in determining the properties of the polymer. Herein, we utilized this UrCy module to design and characterize a novel self-healing material, by incorporating UrCy into a low molecular weight polyurea (PU-UrCy) with polypropylene glycol (PPG) as soft segments and UrCy as hard segments (Scheme 1a). Supramolecular assembly leads to the formation of a physically crosslinked thermoplastic structure with good mechanical properties that is connected by multiple reversible UrCy dimers (Scheme 1b). Importantly, this SPN can be triggered by dynamic interaction of dimerized UrCy moieties, making it highly attractive for rapid re-bonding/dissociation processes. We show that a sudden phase transition is achieved in a very short time frame at the relatively low temperature of 52 °C, which generates an excellent self-healing capability to restore the mechanical and viscoelastic properties of the material under mild conditions. In addition, the interplay between fracture-induced mechanophore activation and noncovalent interactions, as well as the sequence of these mechanical responses, are also demonstrated. To the best of our knowledge, this is the first report of low-molecular-weight supramolecular polymer that can rapidly change its viscoelastic behavior to produce autonomous self-healing materials under mild conditions with good mechanical properties and dimensional stability. Thus, this newly-developed material has significant potential for various applications in regenerative medicine, biomimetic materials and surface engineering.

Experimental section

PU-UrCy and PU were prepared by a combination of Michael addition and condensation polymerization. The general materials, synthetic procedures and instrumentation used in this work are described in more detail in Supplementary Information.

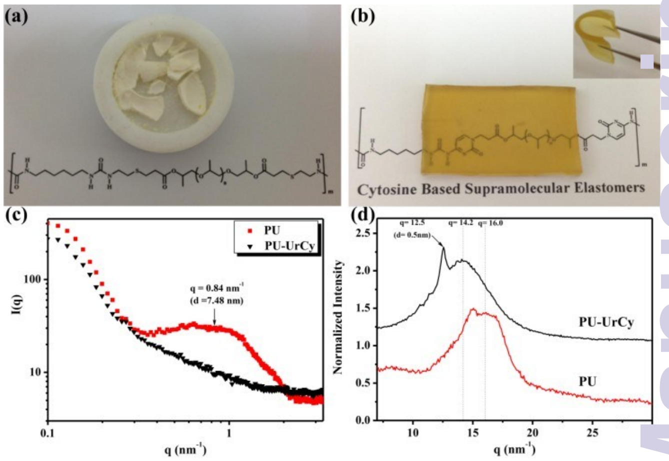

Figure 1. Appearance of **(a)** PU and **(b)** PU-UrCy. The inset photograph in **(b)** shows the flexibility of PU-UrCy film. **(c)** SAXS and **(d)** WAXS data for PU and PU-UrCy recorded at 25 °C.

Results and discussion

Synthesis, microscopic structure and morphological behavior of the UrCy-based supramolecular polymer. A novel multifunctional UrCy macromer created via a simple and efficient two-step synthesis was developed in this study, as illustrated in Scheme S1. Poly(propylene glycol) (PPG) was chosen as the soft segment of the polyurea pre-polymer due to its low glass transition temperature, high hydrophobicity and good environmental durability. A low molecular weight oligomer, cytosine-terminated PPG (Cy-PPG), was obtained by Michael addition of PPG diacrylate 800 (ca. 14 repeat units) reacted with cytosine. The final product was obtained by isocyanate-mediated reaction with Cy-PPG, allowing the preparation of supramolecular PU-UrCy comprising quadruple hydrogen bonding units within the polymer backbone. This innovative approach was successfully exploited and able to achieve high product yields (82.5%), with the resulting PU-UrCy exhibiting an acceptable polydispersity index (PDI = 1.56) and low molecular weight ($M_w = 7120$), as determined by gel permeation chromatography (GPC) (Figure S5). A control polymer, a polyurea without UrCy groups (PU), was also synthesized to enable comparative studies (Scheme S1). When the non-complementary and self-complementary functional groups were incorporated into the polymeric backbone, PU behaved as a powdered solid (Figure 1a) and PU-UrCy appeared as a yellow-colored, translucent, firm, elastic film, respectively, (Figure 1b). This implies that - in the bulk state - the self-complementary motif plays a specific and dominant role in affecting the macroscale properties of supramolecular polymers, prompting us to further investigate the phase behavior in more detail through differential scanning calorimetry (DSC) and small and wide-angle X-ray scattering (SAXS and WAXS) measurements. As shown in Figure S6, the DSC trace of PU-UrCy film underwent a single glass transition (T_g) at -15.4 °C, whereas control PU exhibited two distinct T_gs at -44.2 °C and 70.9 °C indicating the existence of a microphase-separated state. This result demonstrates the critical importance of the UrCy moieties, which can strongly improve the miscibility of PU-UrCy through specific quadruple hydrogen bonding interactions.

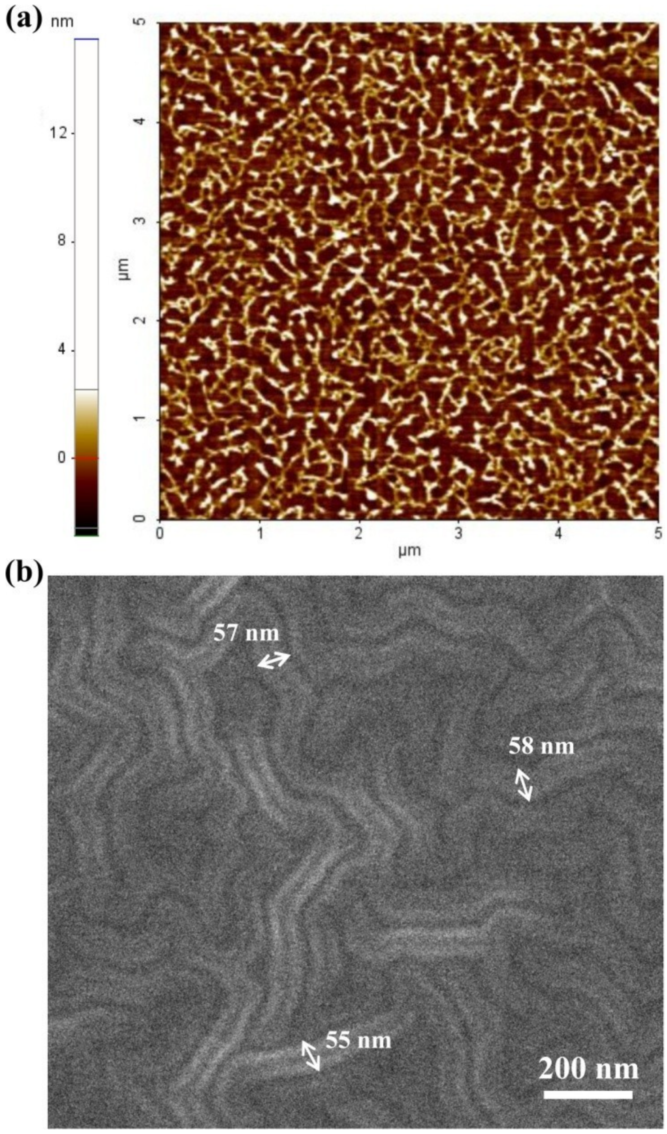

Figure 2. (a) AFM and **(b)** SEM images of spin-coated PU-UrCy film.

To further confirm the DSC results, simultaneous SAXS and WAXS experiments were carried out to analyze the microstructure of the materials (Figures 1c and 1d). The SAXS profiles indicated that PU has a long period peak at q = 0.84 nm^{-1}, corresponding to a spacing of d = 7.48 nm, indicating the occurrence of a phase separation between the hard and soft segments (Figure 1c). However, PU-UrCy behaved as a typical amorphous polymer, implying that the polymer chains tend to be entangled with neighboring chains, resulting in a homogeneous phase in polymer matrices. In other words, PU-UrCy can self-assemble to a highly crosslinked network structure via dynamic interactions between dimerized UrCy moieties, thus improving the compatibility between the hard and soft domains of the PU-UrCy matrix. In the higher q region of the WAXS spectra (Figure 1d), the peak at 12.5 nm^{-1} (d = 0.5 nm) was attributed to the intermolecular distance of the UrCy dimer, i.e., the distance between hydrogen-bonded groups.[42,43] In addition, the amorphous halos of PU-UrCy were obviously shifted to lower *q* values (14.2 nm^{-1}) as compared with PU (q = 16.0 nm^{-1}) indicating the formation of a higher-order hierarchical microstructure with a relatively larger size in PU-UrCy. Comparing the amorphous halos corresponding to the inter-chain distances of PU-UrCy and PU revealed that introduction of the UrCy-UrCy interactions expands the intermolecular main-chain spacing between polymer entanglements and promotes the formation of physically crosslinked networks. Furthermore, the characteristic morphologies of the PU-UrCy and PU films were examined by atomic force microscopy (AFM) and scanning electron microscopy (SEM). Worm-like structures were observed in spin-coated PU-UrCy film (Figures 2a and 2b). The dimensions of the worm-like fibers were uniform, with a length of over 500 nm and constant width of approximately 55 to 58 nm. In contrast, PU formed a typically disordered microphase-separated pattern (Figure S7), implying that the dynamic interactions of UrCy units within the polymer structure promote the formation of hierarchically-ordered structures. In addition, the morphological studies also revealed that PU-UrCy film exhibited a robust SPN, resulting in a well-defined morphology within a fibrous microstructure.

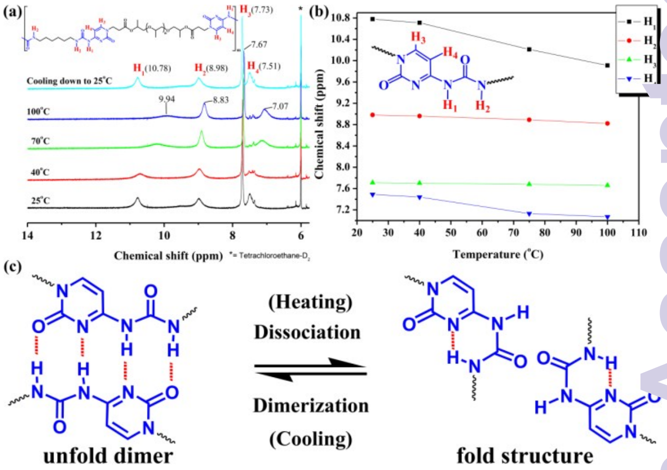

Figure 3. (a) Variable-temperature NMR spectra for a 40 mM solution of PU-UrCy in tetrachloroethane-d_2. **(b)** Temperature dependence of the chemical shift difference (Δδ) between the UrCy protons (H_1-H_4). **(c)** Structural representation of switching between unfolded and folded PU-UrCy structures.

Thermoresponsive solid-viscous switching. In order to understand the stability of the hydrogen bonding interactions within the PU-UrCy system, we performed variable-temperature nuclear magnetic resonance (VT-NMR) experiments in tetrachloroethane-d_2 solution. Figure 3a illustrates the UrCy proton signals for PU-UrCy at 25 °C, in which the characteristic protons were observed at 10.78 (H_1), 8.98 (H_2), 7.71 (H_3) and 7.51 (H_4) ppm, corresponding to the formation of the selective hydrogen bonded complex between UrCy functional groups.[39-41] This result demonstrates that UrCy undergoes highly efficient and directional interactions to build the desired complex. Upon heating from 25 to 100 °C, the protons at H_2 and H_3 did not change apparently; however, the protons at H_1 and H_4 shifted significantly upfield to 9.91 and 7.06 ppm, respectively (Figures 3a and 3b), suggestive of a change in the nature of the hydrogen bonding. We suspect that these effects are possibly a consequence of the equilibrium between unfolded and folded structures (Figure 3c). Increasing the temperature induced a transition from the dynamically-favorable quadruple hydrogen-bonded array (at room temperature) to a kinetically-favorable dual hydrogen-bonded array (at high temperatures). Further investigation of this transition behavior was carried out using rheological measurements (Figure 4a**)**. Dynamic storage modulus (G'), loss modulus (G") and viscosity were plotted against temperature in a double logarithmic format. As the temperature increased above 52 °C, the rheological response of PU-UrCy displayed a sudden phase transition from highly elastic-like (G' > G") behavior to predominantly viscous-like (G" > G') behavior. This phenomenon indicates that a temperature-dependent association between individual UrCy moieties occurs as an interesting phase transition from an amorphous solid to a leather state, in which the UrCy dimers can reversibly rebind, although their recovery remains fragile. At 80 °C, G' became the dominant modulus again, leading to a rubber state in which the material had obvious elastomeric properties. At the same time, the viscosity of PU-UrCy decreased significantly from 1.6×10^5 Pa·s at 40 °C to 1.1×10^4 Pa·s at 80 °C (Figure 4a). When the temperature was increased further to 100 °C, PU-UrCy still maintained a certain amount of viscosity above 5000 Pa·s, suggesting that a small number of crosslinking points were still present within the polymer. This suggestion is supported by the evidence that the hydrogen bonds dissociated and rearranged as temperature increased, suggesting a change in the nature of the hydrogen bond conformation. In other words, the elastic rubber state observed at high temperatures can be attributed to structural folding-induced formation of weak hydrogen-bonded networks (Figure 3c). In contrast, the high modulus presented at low temperatures is presumably a result of the perfect ordering of multiple hydrogen bonds (Figure 3c) formed by construction of a supramolecular polymer with a high cross-linked density. These results also well agree with the VT-NMR data (Figure 3a). To further determine the stability of the structural phase transition, PU-UrCy was cycled between 30 °C and 160 °C in a rheometer (Figures 4b and S8**)**. Even after multiple cycles of cooling and heating, PU-UrCy maintained a conspicuous temperature-dependent response and the elastic modulus and viscosity reverted back perfectly to the original values for each state as temperature decreased; the result of the connection between phase behavior and elastomeric properties. The control PU sample behaved like a plastic material under similar experimental conditions (Figure S9). These observations also revealed that complete reformation of the hydrogen bonding network in PU-UrCy occurred during the cooling periods. Thus, the series of rheological measurements further confirmed the rapid stimuli-responsive behavior and excellent reproducibility of PU-UrCy due to the existence of a reversibly crosslinked network. In addition, it is also noteworthy that the phase transition observed for PU-UrCy occurs under mild conditions, underlining significant potential for rapid, large-scale manufacture of self-healing materials.

Controlling self-healing ability by heat treatment and dynamic interactions. The results described above encouraged us to investigate the self-healing capacity of supramolecular polymers after repetitive breakage-repair cycles. The flexible PU-UrCy sample was placed in a 2 mm-deep mold and subsequently compressed in a heat press at 100 °C and 7 bar for 15 min (Figure 5a), resulting in a transparent, elastic film. Although processing conditions should be maintained at temperatures above 80 °C - the beginning of the rubber state - an operating temperature of 100 °C was chosen based on the rheological data depicted in Figure 4a. At 100 °C, a more complete transformation of the intermolecular hydrogen-bonded conformation was achieved, resulting in a lower viscosity value and thus promoting more rapid healing, while these conditions were sufficiently mild to avoid the negative effects of high temperature on the performance of the material. Figure 5b depicts a typical dynamic mechanical analysis (DMA) thermogram for the original and healed films. During repeated DMA tests, all samples displayed two tan δ peaks at –13 °C and 53 °C, corresponding to the T_g of the thin film and structural phase transitions, respectively. These results were consistent with the DSC and rheological observations: at a temperature above 53 °C, the conformational transition had an appreciable effect on mechanical properties, indicating that PU-UrCy undergoes a rather large elastic deformation during the heating process. When the temperature exceeded 80 °C, the elastomeric film turned into a viscous gel and lost its mechanical properties. However, the 'deformed' samples could be rapidly reshaped in the desired form under mild conditions (100 °C) using a heat press. To date there are no reported examples of self-complementary hydrogen-bonding supramolecular polymers that exhibit rapid recyclability in this manner.

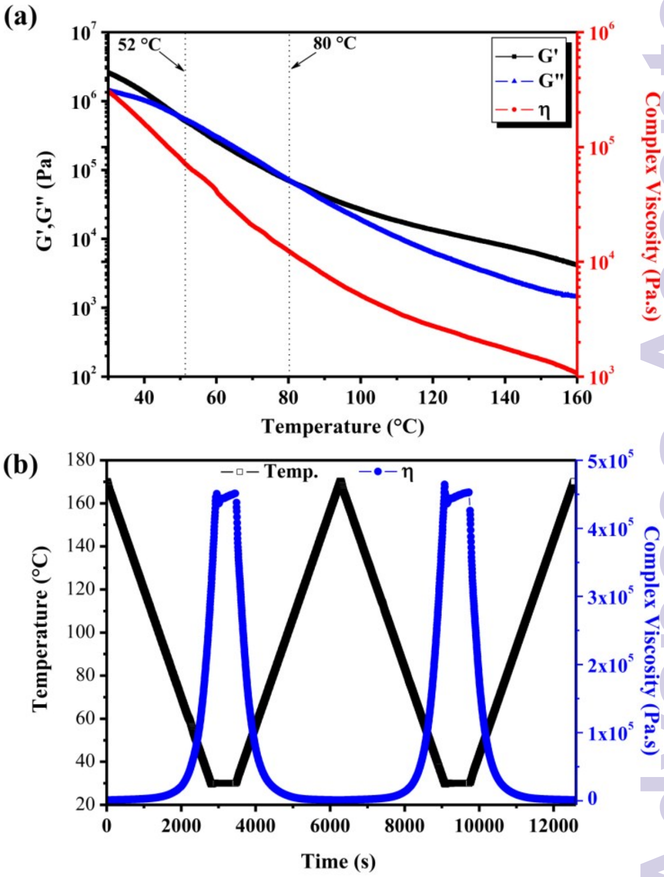

Figure 4. Rheology data for PU-UrCy: **(a)** temperature stability sweep of storage modulus (G'), loss modulus (G") and complex viscosity from 30 to 160 °C. **(b)** Temperature cycling rheology experiments for PU-UrCy: temperature (open symbols) and complex viscosity (solid symbols) variations versus time.

In addition to the observed rapid thermal-dependent reprocessing for de- and re-bonding of the supramolecular network system, we further investigated the self-healing ability of the supramolecular polymer at room temperature conditions without the assistance of an external source. In a typical test procedure, a hot-pressed PU-UrCy film was cut in half with a knife, and then the cut faces were simply contacted at room temperature for different healing times. The tensile strength of the original PU-UrCy sample was 1.17 ± 0.08 MPa with an elongation at break of 390 ± 8% (Figure 6). For all healing times, the mended sample exhibited a time-dependent healing behavior; after 3 h of contact, about 82% of the original strength (0.96 ± 0.04 MPa) had been restored. After 24 h, the mended sample had a tensile strength of 1.15 ± 0.07 MPa and an elongation at break of 243 ± 12%, corresponding to a significant recovery of tensile strength (> 98%) and elongation at break (70%); this is considered to be a relatively high room-temperature healing efficiency for a supramolecular elastomeric material. However, further extending the healing time to 36 h did not further increase the extensibility of the mended sample. This is possibly due to the broken hydrogen bonds exposed on the healing interface becoming increasingly likely to find co-located interaction partners over time, thus inhibiting their availability as intermolecular interactions, while longer healing times are required to increase mechanical properties. In order to confirm these results, the effect of time on the healing process was observed using SEM according to the sample preparation routine described above. The SEM images demonstrated that the cracks between the fracture surfaces were almost completely healed after healing at room temperature for 16 h (Figure S10), in confirmation of autonomic self-healing ability as well as a rapid dynamic response to mechanical recovery. These studies also confirmed that the dynamics of multiple hydrogen bonding environments are responsible for the strength and extensibility of supramolecular films and are essential to promote multiple healing actions.

Conclusions

In summary, we have demonstrated a simple and effective strategy for developing rapidly repairable and stimuli-responsive materials with improved long-term durability. Incorporating the quadruple hydrogen bonding UrCy motifs into the polymer backbone provides a simple self-assembly route towards the formation of a physically crosslinked polymer network. Due to the presence of a reversible network and the homogeneity of the crosslinks, the supramolecular polymer could be reshaped and reprocessed by hot pressing under mild conditions - a result of rearrangement of the hydrogen bond conformation during the hot-pressing process. Moreover, this material can also undergo self-healing at room temperature without external intervention, as evidenced by the gradual restoration of mechanical properties over time. Thus, the material developed in this study is not only able to support rapid reprocessing of damage during mild heat-treatment (100 °C), but is also able to dynamically repair the mechanical properties of fractured samples at room temperature, making it particularly appealing for the development of high-efficiency self-healing materials. While the main focus of the current study was to explore a supramolecular design strategy for self-healing materials, we envision that this strategy could be applied in a wide variety of practical applications, especially tissue materials and regenerative medicine; these aspects are currently being investigated in our laboratory.

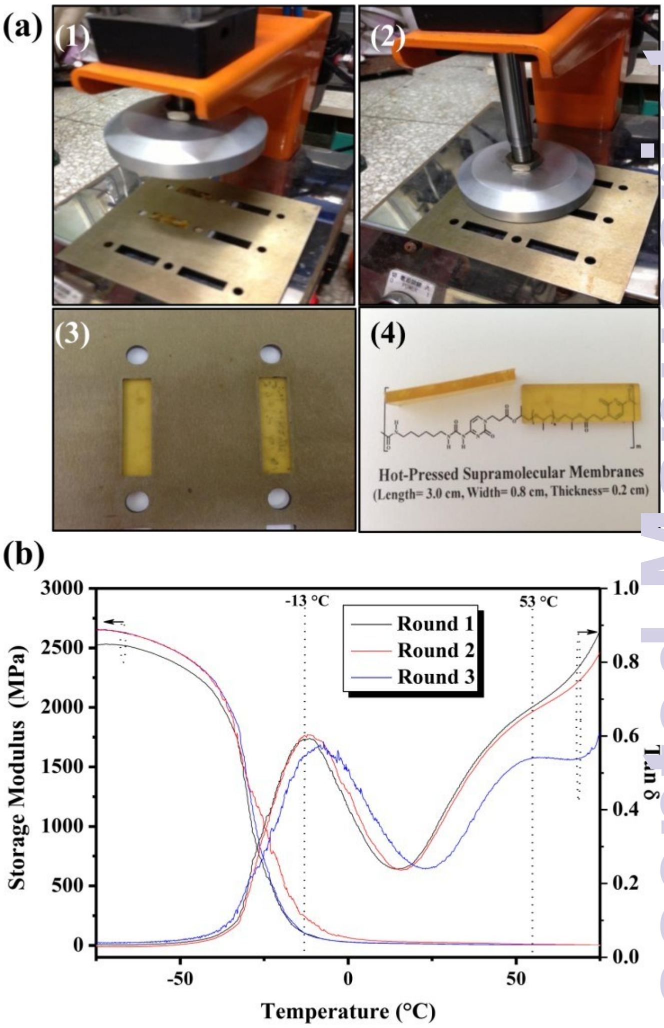

Figure 5. **(a)** A rapid reprocessing of PU-UrCy through hot-pressing at 100 °C and 7 bar for 15 min (1 and 2). After that time, the polymer was reshaped in the form of a transparent film (3 and 4). **(b)** DMA curves for original and healed PU-UrCy subjected to successive breakage and reshaping procedures.

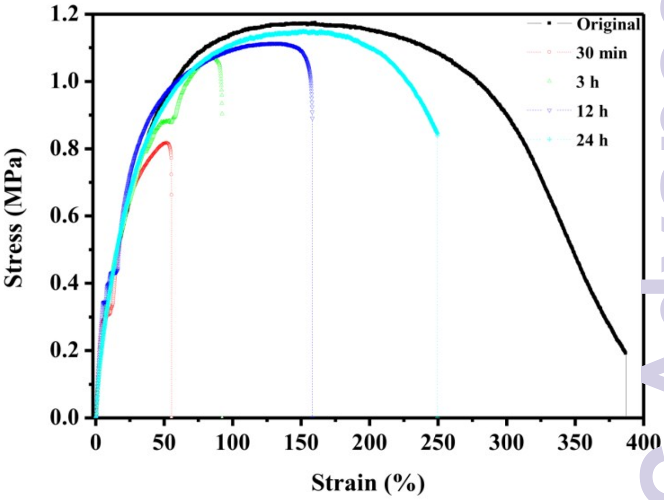

Figure 6. Stress-strain curves for original and healed PU-UrCy films. The hot-pressed films were cut in half with a knife and the cut faces were gently contacted at 25 °C for different healing times.

Acknowledgements

This study was supported financially by "Aim for the Top University Plan" of the National Taiwan University of Science and Technology, and the Ministry of Science and Technology, Taiwan (contract no. MOST 104-2221-E-011-153).

Notes and references

1 M. D. Hager, P. Greil, C. Leyens, S. van Der Zwaag and U. S. Schubert, *Adv. Mater.*, 2010, **22**, 5424–5430.

2 S. Burattini, B. W. Greenland, D. Chappell, H. M. Colquhoun and W. Hayes, *Chem. Soc. Rev.*, 2010, **39**, 1973–1985.

3 B. K. Ahn, D. W. Lee, J. N. Israelachvili and J. H. Waite. *Nature materials*, 2014, **13**, 867–872.

4 S. R. White, J. S. Moore, N. R. Sottos, B. P. Krull, W. A. Santa Cruz and R. C. R. Gergely, *Science*, 2014, **344**, 620–623.

5 X. K. D. Hillewaere and F. E. Du Prez, *Prog. Polym. Sci.*, 2015, dx.doi.org/10.1016/j.progpolymsci.2015.04.004.

6 N. Roy, B. Bruchmann and J.-M. Lehn, *Chem. Soc. Rev.*, 2015, **44**, 3786–3807.

7 P. Cordier, F. Tournilhac, C. Soulie-Ziakovic and L. Leibler, *Nature*, 2008, **451**, 977–980.

8 B. Ghosh and M.W. Urban, *Science*, 2009, **323**, 1458–1460.

9 Y. Amamoto, J. Kamada, H. Otsuka, A. Takahara and K. Matyjaszewski, *Angew. Chem.*, 2011, **123**, 1698–1701.

10 B. J. Blaiszik, S. L. Kramer, M. E. Grady, D. A. McIlroy, J. S. Moore, N. R. Sottos and S. R. White, *Adv. Mater.*, 2012, **24**, 398–401.

11 E. Palleau, S. Reece, S. C. Desai, M. E. Smith and M. D. Dickey, *Adv. Mater.*, 2013, **25**, 1589–1592.

12 C. Wang, H. Wu, Z. Chen, M. T. McDowell, Y. Cui and Z. Bao, *Nature Chemistry*, 2013, **5**, 1042–1048.

13 Z. Zhao and E. M. Arruda, *Science*, 2014, **344**, 591–592.

14 A. Phadke, C. Zhang, B. Arman, C. C. Hsu, R. A. Mashelkar, A. K. Lele, M. J. Tauber, G. Arya and S. Varghese, *Proc. Natl. Acad. Sci. USA*, 2012, **109**, 4383–4388.

15 X. Yu, L. Chen, M. Zhang and T. Yi , *Chem. Soc. Rev.*, 2014, **43**, 5346–5371.

16 M. A. C. Stuart, *Nature Mater.*, 2010, **9**, 101–113.

17 (a) X. Yan, F. Wang, B. Zheng and F. Huang, *Chem. Soc. Rev.*, 2012, **41**, 6042–6065.; (b) S. Y. Dong, B. Zheng, F. Wang and F. H. Huang, Acc. Chem. Res., 2014, **47**, 1982–1994.

18 S. R. White, N. R. Sottos, P. H. Geubelle, J. S. Moore, M. R. Kessler, S. R. Sriram, E. N. Brown and S. Viswanathan, *Nature*, 2001, **409**, 794–797.

19 X. Chen, M. A. Dam, K. Ono, A. Mal, H. Shen, S. R. Nutt, K. Sheran and F. Wudl, *Science*, 2002, **295**, 1698–1702.

20 P. Zheng and T. J. McCarthy, *J. Am. Chem. Soc.*, 2012, **134**, 2024–2027.

21 K. Imato, M. Nishihara, T. Kanehara, Y. Amamoto, A. Takahara and H. Otsuka, *Angew. Chem. Int. Ed.*, 2012, **124**, 1164–1168.

22 K. K. Oehlenschlaeger, J. O. Mueller, J. Brandt, S. Hilf, A. Lederer, M. Wilhelm, R. Graf, M. L. Coote, F. G. Schmidt and C. Barner-Kowollik, *Adv. Mater.*, 2014, **26**, 3561–3566.

23 R Martin, A. Rekondo, A. R. de Luzuriaga, G. Cabañero, H. J. Grandea and I. Odriozola, *J. Mater. Chem. A*, 2014, **2**, 5710–5715.

24 M. Burnworth, L. Tang, J. R. Kumpfer, A. J. Duncan, F. L. Beyer, G. L. Fiore, S. J. Rowan and C. Weder, *Nature*, 2011, **472**, 334–337.

25 N. Holten-Andersen, M. J. Harrington, H. Birkedal, B. P. Lee, P. B. Messersmith, K. Y. C. Lee and J. H. Waite, *Proc. Natl. Acad. Sci. USA*, 2011, **108**, 2651–2655.

26 S. Burattini, H. M. Colquhoun, J. D. Fox, D. Friedmann, B. W. Greenland, P. J. F. Harris, W. Hayes, M. E. Mackay and S J. Rowan, *Chem. Commun.* 2009, 6717-6719.

27 D. Montarnal, F. Tournilhac, M. Hidalgo, J.-L. Couturier and L. Leibler, *J. Am. Chem. Soc.*, 2009, **131**, 7966–7967.

28 A. B. South and L. A. Lyon, *Angew. Chem. Int. Ed.*, 2010, 49, 767–771.

29 S. Burattini, B. W. Greenland, D. H. Merino, W. Weng, J. Seppala, H. M. Colquhoun, W. Hayes, M. E. Mackay, I. W. Hamley and S. J. Rowan, *J. Am. Chem. Soc.*, 2010, **132**, 12051–12058.

30 Q.Wang, J. L. Mynar, M. Yoshida, E. Lee, M. Lee, K. Okuro, K. Kinbara and T. Aida, *Nature*, 2010, **463**, 339–343.

31 Y. Chen, A. M. Kushner, G. A. Williams and Z. Guan, *Nature Chem.*, 2012, **4**,467–472.

32 (a) M. M. Zhang, D. H. Xu, X. Z. Yan, J. Z. Chen, S. Y. Dong, B. Zheng and F. H. Huang, *Angew. Chem. Int. Ed.*, 2012, **124**, 7117–7121.; (b) X. Z. Yan, D. H. Xu, J. Z. Chen, M. M. Zhang, B. J. Hu, Y. H. Yu and F. Huang, *Polym. Chem.*, 2013, **4**, 3312-3322.

33 J. Cui and A. del Campo. *Chem. Commun.*, 2012, **48**, 9302–9304.

34 (a) F. Herbst, S. Seiffert and W. H. Binder, *Polym. Chem.*, 2012, **3**, 3084–3092.; (b) R. Zhang, T. Yan, B.-D. Lechner, K. Schröter, Y. Liang, B. Li, F. Furtado, P. Sun and K. Saalwächter, *Macromolecules*, 2013, **46**, 1841–1850.; (c) C. Wang, N. Liu, R. Allen, J. B. Tok, Y. Wu, F. Zhang, Y. Chen and Z. Bao, *Adv. Mater.*, 2013, **25**, 5785–5790.

35 (a) P. Reutenauer, E. Buhler, P. J. Boul, S. J. Candau and J. M. Lehn, *Chem. Eur. J.*, 2009, **15**, 1893–1900.; (b) N. R. Sottos and J. S. Moore, *Nature*, 2011, **472**, 299–300.

36 (a) R. F. M. Lange, M. Van. Gurp and E. W. Meijer, *J. Polym. Science: Part A,. Polym. Chem.*, 1999, **37**, 3657–3670.; (b) S. Seiffert and J. Sprakel, *Chem. Soc. Rev.*, 2012, **41**, 909–930.; (d) M. Guo, L. M. Pitet, H. M. Wyss, M. Vos, P. Y. W. Dankers and E. W. Meijer, *J. Am. Chem. Soc.*, 2014, **136**, 6969–6977.; (c) P. F. Wei, X. Z. Yan and F.H. Huang, *Chem. Soc. Rev.*, 2015, **44**, 815–832.

37 S. K. Yang and S. C. Zimmerman, *Isr. J. Chem.*, 2013, **53** 511–520.

38 L. Yang , X. Tan , Z. Wang and X. Zhang, *Chem. Rev.*, 2015, **115**, 7196–7239.

39 V. G. H. Lafitte, A. E. Aliev, P. N. Horton, M. B. Hursthouse, K. Bala, P. Golding and H. C. Hailes, *J. Am. Chem. Soc.*, 2006, **128**, 6544–6545.

40 E. Greco, A. E. Aliev, V. G. H. Lafitte, K. Bala, D. Duncan, L. Pilon, P. Golding and H. C. Hailes, *New J. Chem.*, 2010. **34**, 2634–2642.

41 C. C. Cheng, F. C. Chang, J. H. Wang, Y. L. Chu, Y. S. Wang, D. J. Lee, W. T. Chuang and Z. Xin, *RSC Adv.*, 2015, **5**, 76451–76457.

42 S. J. George and A. Ajayaghosh, *Chem. Eur. J.*, 2005, **11** 3217–3227.

43 S. Sivakova, D. A. Bohnsack, M. E. Mackay, P. Suwanmala and S. J. Rowan, *J. Am. Chem. Soc.*, 2005, **127**, 18202–18211

Table of Contents

A new urea-cytosine-functionalized supramolecular polymer can be rapidly reshaped and reprocessed under mild conditions via rearrangement of the hydrogen bonding network.